

Analysis of axisymmetric shells based on the scaled boundary finite element method

Milan Wallner^{1*}, Carolin Birk¹ and Hauke Gravenkamp¹

Micro Abstract

In this contribution the SBFEM is used to analyse axisymmetric shell structures. A simplified plane strain arch formulation to approximate a cylindrical shell will be presented. This approximation already shows a high correlation with the membrane theory of shells. Furthermore, first results obtained for a 3D shell formulation used to analyse an axisymmetric spherical shell will illustrate the potential of the SBFEM to minimize locking effects when modelling shell structures.

¹Institute of Structural Analysis of Plates and Shells, University of Duisburg-Essen, Essen, Germany

*Corresponding author: milan.wallner@uni-due.de

Introduction

Numerical modelling of shell structures is still a subject of high interest to this day. This sustained interest is due to a variety of reasons. Firstly, shell structures can be found in many structural engineering applications. In general, the structural behaviour of shells is analysed numerically, since complex shell geometries limit the applicability of analytical solutions. The primary reason, however, is the occurrence of locking effects when using conventional finite elements. Shell elements are affected by membrane locking as well as shear locking, with membrane locking being more dominant. These locking effects result in an overly stiff behaviour of the numerical model. Shear locking means zero transverse shear strains cannot be accurately represented. On the other hand, membrane locking is associated with failure to represent the state of zero membrane strains in curved structures. Both locking effects increase as the shell thickness decreases. Approaches to avoid locking of shell structures include reduced integration, discrete strain gap formulation, assumed natural strain approaches and enhanced assumed strain methods.

The scaled boundary finite element method (SBFEM) combines the advantages of the finite element method and the boundary element method. In this semi-analytical approach, the spatial dimension is reduced by one through only discretizing the boundary of the domain. This semi-discretization process results in a set of ordinary differential equations which can be solved analytically in order to obtain the static stiffness matrix. Plate elements based on the SBFEM have already been developed and been shown to successfully avoid shear locking completely [1,2]. The principal approach for these elements is to discretize only the mid-surface and to solve analytically in the through-thickness direction. Locking effects of shells are heavily dependent on the thickness of the structure, therefore the SBFEM seems to be a promising method to develop elements that show reduced locking effects for shells since the through-thickness direction is handled analytically. The present work reports first studies on the development of SBFEM-based shell elements in the form of a numerical example for a spherical zone shell under constant pressure.

1 The scaled boundary finite element method

The derivation of the scaled boundary finite element method starts with the choice of the so-called scaling center O , from where the whole boundary must be visible. The dimensionless

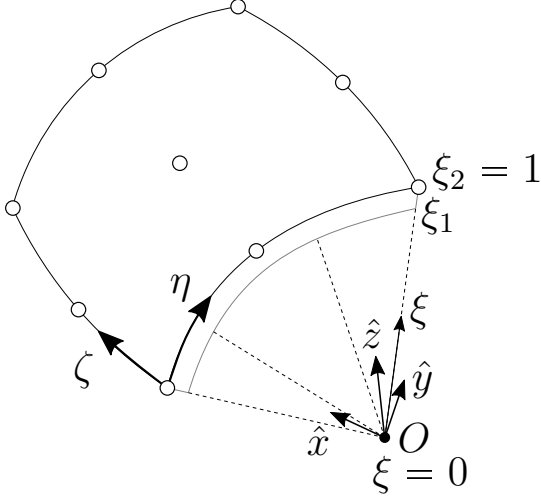


Figure 1. Scaled boundary local coordinates

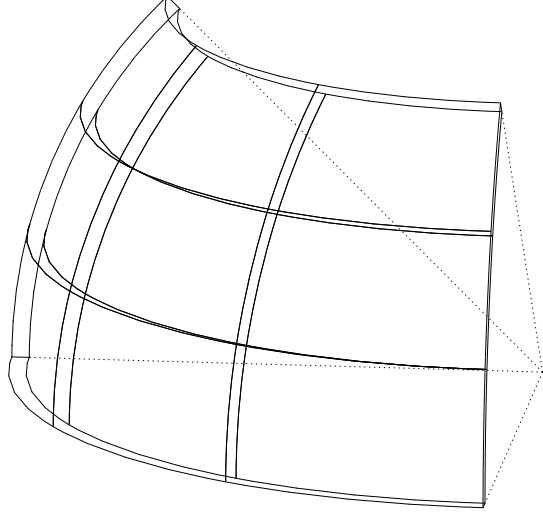


Figure 2. Spherical zone shell

local coordinates η , ζ and ξ are introduced to describe the domain. Here, the local coordinates η and ζ describe the circumferential directions of the boundary. The coordinate ξ points from the scaling center O in radial direction towards the boundary, with $\xi = 0$ at the scaling center O and $\xi = 1$ on the boundary (see Figure 1). Interpolating the nodal coordinates $\{x_n\}$, $\{y_n\}$ and $\{z_n\}$ using the shape functions $[N(\eta, \zeta)]$ and scaling the geometry of the boundary, the geometry of the domain is mapped from Cartesian coordinates to local scaled boundary coordinates. This process is called the *scaled boundary coordinate transformation*.

$$\hat{x}(\xi, \eta, \zeta) = \xi[N(\eta, \zeta)]^T \{x_n\}, \quad \hat{y}(\xi, \eta, \zeta) = \xi[N(\eta, \zeta)]^T \{y_n\}, \quad \hat{z}(\xi, \eta, \zeta) = \xi[N(\eta, \zeta)]^T \{z_n\}. \quad (1)$$

The *scaled boundary finite-element equation in displacement* can be derived using the weighted residual technique [4] or the principle of virtual work [1]. For 3D problems the *scaled boundary finite-element equation in displacement* (2) reads

$$[E^0]\xi^2\{u(\xi)\}_{,\xi\xi} + (2[E^0] + [E^1]^T - [E^1])\xi\{u(\xi)\}_{,\xi} + ([E^1]^T - [E^2])\{u(\xi)\} = 0, \quad (2)$$

with the *coefficient matrices* $[E^0]$, $[E^1]$ and $[E^2]$ (3)-(5). The *coefficient matrices* are obtained by numerical integration along the circumferential directions η and ζ and depend on the *scaled boundary transformation* of the elastic strains $[B^1]$ and $[B^2]$ as well as on the elasticity matrix $[D]$.

$$[E^0] = \int_S [B^1]^T [D] [B^1] |J| d\eta d\zeta \quad (3)$$

$$[E^1] = \int_S [B^2]^T [D] [B^1] |J| d\eta d\zeta \quad (4)$$

$$[E^2] = \int_S [B^2]^T [D] [B^2] |J| d\eta d\zeta \quad (5)$$

The *scaled boundary finite-element equation in displacement* (2) can be transformed into a system of first-order ordinary differential equations

$$\xi\{X(\xi)\}_{,\xi} = -[Z]\{X(\xi)\}, \quad [Z] = \begin{bmatrix} [E^0]^{-1}[E^1]^T - 0.5[I] & -[E^0]^{-1} \\ -[E^2] + [E^1][E^0]^{-1}[E^1]^T & -([E^1][E^0]^{-1} - 0.5[I]) \end{bmatrix}, \quad (6)$$

where $\{X(\xi)\}$ contains the nodal displacements $\{u(\xi)\}$ and nodal forces $\{q(\xi)\}$ on the boundary,

$$\{X(\xi)\} = \begin{Bmatrix} \xi^{0.5}\{u(\xi)\} \\ \xi^{-0.5}\{q(\xi)\} \end{Bmatrix}. \quad (7)$$

The general solution of the system of first-order ordinary differential equations (6) can be written as [3],

$$\{X(\xi)\} = [\Psi]\xi^{-[S]}\{c\}, \quad (8)$$

with $[S]$ being the block diagonalized Schur decomposition of the matrix $[Z]$ containing the eigenvalues of $[Z]$ on the main diagonal. $[\Psi]$ is a transformation matrix which also results from the Schur decomposition of the matrix $[Z]$ and $\{c\}$ are integration constants. Separating the solutions for the nodal displacements $\{u(\xi)\}$ and forces $\{q(\xi)\}$ leads to the expressions

$$u(\xi) = \xi^{-0.5} \left([\Psi_{u1}]\xi^{-[S_n]}\{c_1\} + [\Psi_{u2}]\xi^{-[S_p]}\{c_2\} \right), \quad (9)$$

$$q(\xi) = \xi^{0.5} \left([\Psi_{q1}]\xi^{-[S_n]}\{c_1\} + [\Psi_{q2}]\xi^{-[S_p]}\{c_2\} \right). \quad (10)$$

In order to describe a thin shell structure, we now introduce the inner and outer boundaries of the shell structure. The radial coordinate at the inner boundary is denoted as ξ_1 and satisfies $0 \leq \xi_1 < 1$, depending on the ratio between shell thickness and radius, while the outer boundary is described by $\xi_2 = 1$. Substituting the values ξ_1 and ξ_2 into the solutions for the nodal displacements and forces (9)-(10), these can be expressed as

$$\begin{Bmatrix} \{u_1\} \\ \{u_2\} \end{Bmatrix} = \begin{bmatrix} \xi_1^{-0.5[I]}\Psi_{u1}\xi_1^{-[S_n]} & \xi_1^{-0.5[I]}\Psi_{u2} \\ \Psi_{u1} & \Psi_{u2}\xi_1^{[S_p]} \end{bmatrix} \begin{Bmatrix} \{c_1\} \\ \{c_2\} \end{Bmatrix}, \quad (11)$$

$$\begin{Bmatrix} \{q_1\} \\ \{q_2\} \end{Bmatrix} = \begin{bmatrix} \xi_1^{0.5[I]}\Psi_{q1}\xi_1^{-[S_n]} & \xi_1^{0.5[I]}\Psi_{q2} \\ \Psi_{q1} & \Psi_{q2}\xi_1^{[S_p]} \end{bmatrix} \begin{Bmatrix} \{c_1\} \\ \{c_2\} \end{Bmatrix}. \quad (12)$$

Due to numerical difficulties when evaluating the expression $\xi^{-[S_p]}$ for large eigenvalues, the integration constant $\{c_2\}$ is substituted with $\{d_2\} = \xi^{-[S_p]}\{c_2\}$ leading to $\{c_2\} = \xi^{[S_p]}\{d_2\}$. The static stiffness matrix relating nodal displacements and external forces is defined as

$$\begin{Bmatrix} \{f_i\} \\ \{f_e\} \end{Bmatrix} = [K] \begin{Bmatrix} \{u_i\} \\ \{u_e\} \end{Bmatrix}. \quad (13)$$

Rearranging (13) and using the relation between internal and external forces $\{f_i\} = -\{q_i\}$ results in the static stiffness matrix

$$[K] = \begin{bmatrix} -\xi_1^{-0.5[I]}\Psi_{q1}\xi_1^{-[S_n]} & -\xi_1^{-0.5[I]}\Psi_{q2} \\ \Psi_{q1} & \Psi_{q2}\xi_1^{[S_p]} \end{bmatrix} \begin{bmatrix} \xi_1^{-0.5[I]}\Psi_{u1}\xi_1^{-[S_n]} & \xi_1^{-0.5[I]}\Psi_{u2} \\ \Psi_{u1} & \Psi_{u2}\xi_1^{[S_p]} \end{bmatrix}^{-1}. \quad (14)$$

2 Numerical example

The proposed technique was tested for an axisymmetric spherical zone shell under constant pressure (see Figure 2). The opening angle is 45° with a radius of $1.5 m$ while the thickness is varied between $0.3 m$ and $0.0001 m$. Only one-quarter of the shell was modelled while the remaining three-quarters were taken into account by symmetry boundary conditions. The radial deflection at the bottom of the shell was calculated. The numerically obtained results are evaluated with respect to the analytical solution for the membrane state of stress for the present example. The spherical zone shell was examined with respect to several aspects. The system was modelled using different methods: e.g. the SBFEM, solid elements as well as linear and quadric shell elements in Ansys.

Figure 3 shows the relative error with respect to the analytical solution (for the membrane state of stress) of the radial deflection of the spherical zone shell at the bottom. The system has been analysed using shell and solid elements in Ansys as well as p- and h-refinement for the SBFEM.

The results demonstrate that the SBFEM solutions based on high-order approximations converge closer to the analytical solution with fewer degrees of freedom than the elements provided by Ansys. The strong influence of the thickness on the accuracy of the different methods can be seen in Figure 4. The Ansys shell elements yield a smaller error than the other methods for higher thicknesses. This is due to the fact that none of the other approaches is based on the assumption that stresses in the through-thickness direction are equal to zero, which is an essential part of the thin shell theory. With reducing thickness this effect is minimized and the other methods yield smaller errors. However, all the methods used yield less accurate results as the thickness is decreased further, to a point where its physical reasonability can be questioned. Investigations of this effect are ongoing. One possible explanation could be that the assumption of small deformations used in the thin shell theory is no longer applicable for very low thickness-radius ratios.

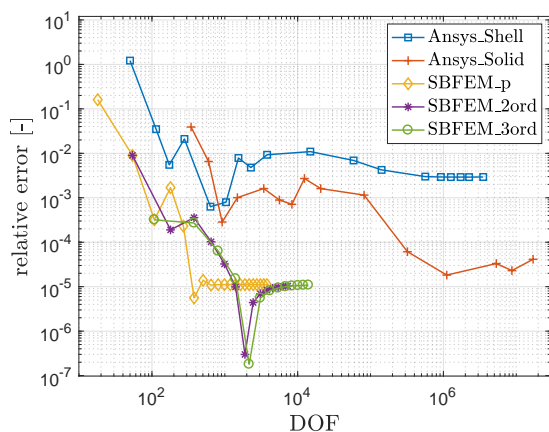


Figure 3. Convergence of radial deflection at the bottom for $t/R = 0.01$

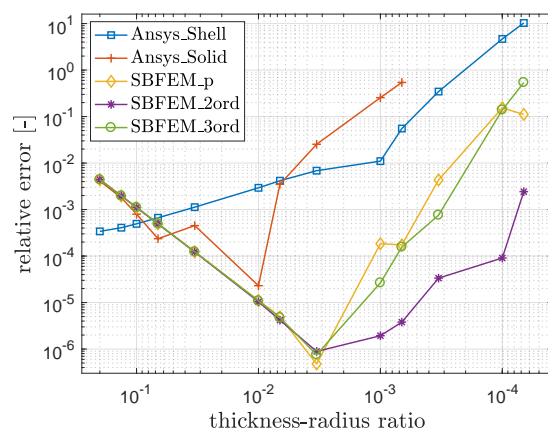


Figure 4. Convergence of radial deflection at the bottom for several thickness-radius ratios

Conclusions

The proposed technique shows promising results by reaching higher accuracy compared to conventional FEA. Additional studies regarding linear shape functions are ongoing. Further, a numerical example including bending will be studied in order to investigate membrane locking since the latter effect mainly occurs when membrane and bending action are coupled.

References

- [1] H. Man, C. Song, W. Gao, and F. Tin-Loi. A unified 3D based technique for plate bending analysis using scaled boundary finite element method. *Int. J. Numer. Methods Eng.*, 91:491–515, 2012.
- [2] H. Man, C. Song, T. Xiang, W. Gao, and F. Tin-Loi. High-order plate bending analysis based on the scaled boundary finite element method. *Int. J. Numer. Methods Eng.*, 95:331–360, 2013.
- [3] C. Song. A matrix function solution for the scaled boundary finite-element equation in statics. *Comput. Methods Appl. Mech. Eng.*, 193:2325–2356, 2004.
- [4] C. Song and J. P. Wolf. The scaled boundary finite-element method: analytical solution in frequency domain. *Comput. Methods Appl. Mech. Eng.*, 164:249–264, 1998.